LATEST RESULTS FROM THE ITER H-MODE CONFINEMENT AND THRESHOLD DATABASES.

K. THOMSEN[6], G. BRACCO[5], C. BUSH[8], T.N. CARLSTROM[4], A.N. CHUDNOVSKII[9], J.G. CORDEY[6], J.C. DEBOO[4], S.J. FIELDING[3], T. FUKUDA[7], M. GREENWALD[1], G.T. HOANG[11], A. HUBBARD[1], Y. KAMADA[7], O.J.W.F. KARDAUN[2], S.M. KAYE[8], A. KUS[2], C. LOWRY[6], Y. MARTIN[12], T. MATSUDA[7], Y. MIURA[7], J. ONGENA[10], E. RIGHI[13], F. RYTER[2], D.P. SCHISSEL[4], J.A. SNIPES[1], W. SUTTROP[2], T. TAKIZUKA[7], H. TAMAI[7], K. TSUCHIYA[7], M. VALOVIC[3], ALCATOR C-MOD TEAM[1], ASDEX TEAM[2], ASDEX UPGRADE TEAM[2], COMPASS-D TEAM[3], DIII-D TEAM[4], FTU TEAM[5], JET TEAM[6], JFT-2M TEAM[7], JT-60U TEAM[7], PBX-M TEAM[8], PDX TEAM[8], T-10 TEAM[9], TCV TEAM[12], TEXTOR TEAM[10], TFTR TEAM[8], TORE-SUPRA TEAM[11].

1. Plasma Science and Fusion Center, MIT, USA.
2. Max-Planck-Institute for Plasma Physics, Garching, Germany.
3. United Kingdom Atomic Energy Authority, Culham, UK.
4. General Atomics, San Diego, USA.
5. ENEA Frascati Energy Research Center, Frascati, Italy.
6. JET Joint Undertaking, Abingdon, UK.
7. Japan Atomic Energy Research Institute, Naka, Japan.
8. Princeton Plasma physics Laboratory.
9. Russian Research Center Kurchatov Institute, Moscow.
10. ERM/KMS - EURATOM, Belgium State, Belgium.
11. Centre d'Etudes Nucleaires de Cadarache, Cadarache, France.
12. CRPP/EPFL, Lausanne, Switzerland.
13. NET Team, Garching, Germany.

Abstract

New H-mode power threshold scaling expressions have been found which incorporates an assumed 1/M isotope dependence for hydrogenic plasmas. Preliminary power threshold predictions based on discriminant analysis have also been made. However, the ITER predictions are still uncertain. The log-linear confinement scaling expressions suggest that the L-mode is governed by Bohm type transport whereas the ELMY H-mode is governed by gyro-Bohm transport. Various non-linear scalings also fit the ELMy H-mode data and a confidence interval for the predicted confinement time in ITER has been established which takes the predictions of these into account

1. INTRODUCTION

The ITER H-mode Power Threshold, L-mode and H-mode Confinement Databases [1-3] have all been expanded with new data in the last two years and the number of contributing tokamaks has increased. Here some of the recent findings using these databases will be presented, see also [4-6].

2. H-MODE THRESHOLD POWER

The ITER Threshold Database contains data from 10 divertor tokamaks (ASDEX, ASDEX Upgrade, Alcator C-Mod, COMPASS-D, DIII-D, JET, JFT-2M, JT-60U, PBX-M and TCV). Since the previous IAEA conference [7] efforts have been made to understand the causes of the large scatter of the data and to improve the quality of the database by adding new data.

Regressions on the points just at the L-H transition yield the following two expressions (units of M, n_{20}, S, P_{thres}, B, R and a are AMU, 10^{20} m^{-3}, m^2, MW, T, m and m, respectively):

$$P_{thres} = 0.082\, M^{-1.0}\, n_{20}^{0.69}\, B^{0.91}\, S^{0.96}, \qquad \text{RMSE} = 25.2\% \qquad (1)$$

$$P_{thres} = 2.76\ M^{-1.0}\ n_{20}^{0.77}\ B^{0.92}\ R^{1.30}\ a^{0.76}\ , \qquad RMSE = 25.1\% \qquad (2)$$

The data from ASDEX (only circular device), COMPASS-D and TCV (smallest devices with an open divertor) have not been included in the regressions because they are above the prediction according to both regression models, see e.g. Fig.1. For the latter 2 devices neutrals may be the cause of the increased power threshold. Both Eqs. (1) and (2) are dimensionally correct within the uncertainties of the exponents. The dependence on S is in agreement with the L-H transition being an edge phenomenon. The expressions were obtained from deuterium data. The dependence on M is only valid for hydrogenic plasmas and was imposed based on operation in hydrogen and deuterium as well as tritium [8]. The extrapolated values for ITER using Eqs.(1) and (2) are 85 (56 - 153) MW and 107 (63 - 179) MW, respectively. The uncertainty on P_{thres} is largely due to data scatter that can reach a factor of 2 within a single device. The data scatter has several causes that vary from device to device. One effect is wall conditioning, the threshold being higher in high recycling cases. It has been shown in several devices that the edge electron temperature is almost constant for given values of B and I. Therefore, to reach the required temperature, more heating power is necessary at higher edge density (i.e. high recycling). Using the edge density instead of the line-averaged density in the analysis would be preferable. However, the lack of data and the large scatter of the available measurements have prevented a reliable result to be obtained. Moreover, the edge density in ITER is not known with accuracy. Therefore, at present, using the edge density does not improve the prediction. A second cause for scatter in several devices is due to the sawteeth. The heat pulse following a sawtooth crash can trigger the L-H transition when it reaches the edge. Depending on the plasma conditions and time evolution of the discharge, the L-H transition may be triggered by a sawtooth heat pulse with variable efficiency or not at all. Presently it is not possible to reliably take this effect into account, but modeling is being carried out. A cause of data scatter in Alcator C-Mod is attributed to the variation of the ICRH absorption. A correction to the heating power with experimental absorption factors has decreased the scatter and reduced the density dependence in this device. However, the overall results did not change significantly.

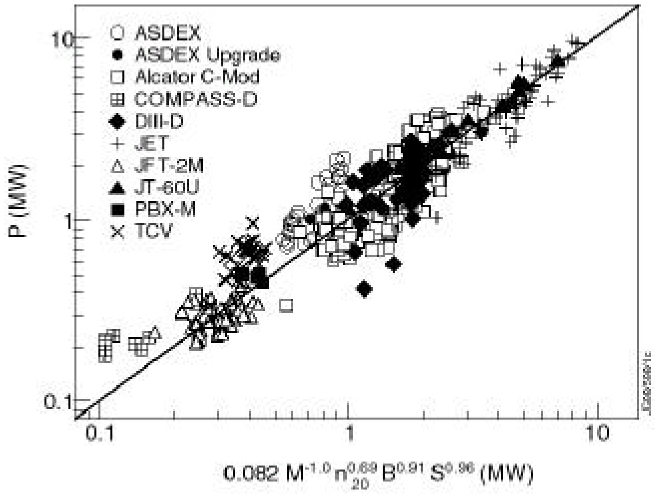

Fig. 1. Comparison of experimental power thresholds with scaling expression Eq.(1).

Discriminant Analysis is used to determine a set of hyperplanes in a multidimensional space, which best separates two classes of data. An investigation of the H-mode power threshold using this approach has been initiated [5]. The first class consists of L-mode data and the second of H-mode data. In order to increase the number of data points all 3 databases (L-mode, H-mode and Threshold database) have been merged together. However, only data from tokamaks contributing both L-mode and H-mode data have been considered. The resulting dataset is thus significantly different from the one used in the previous section. R, B, κ, q_{95}, n and the loss power P constitute the multidimensional space. The discriminant function (constant on each hyperplane) can be transformed into a function that gives the probability of a data point to belong to the H-mode class. With this model about 75% of the data are well classified. The model can be used to predict the H-mode threshold power in the following way. For design values of R, B, κ, q_{95} and n, the loss power P is increased until the model shows a probability larger than 0.5. That value of P is considered to be the threshold power. The prediction for ITER is 80 (25 - 200) MW. Threshold predictions for independent scans of R, B, κ, q_{95} and n have also been calculated. They show that this model is equivalent to a threshold power scaling which increases with R, B and κ but decreases with q_{95} and n. The latter dependence is not in agreement with the results obtained by regression analysis and hence deserves further consideration.

3. L-MODE CONFINEMENT

The present public L-mode database consists of data from 14 tokamaks (Alcator C-Mod, ASDEX, DIII, DIII-D, FTU, JET, JFT-2M, JT-60U, PBX-M, PDX, TEXTOR, TFTR, Tore-Supra, and T-10). In [4] a dimensionally correct fit to the thermal confinement data for the combined limiter and divertor data subsets is given (in units of s, MA, T, MW, 10^{19}m^{-3}, AMU, m, -, -):

$$\tau_{th}^{ITERL97P} = 0.023\ I^{0.96}\ B^{0.03}\ P^{-0.73}\ n_{19}^{0.40}\ M^{0.20}\ R^{1.83}\ \varepsilon^{-0.06}\ \kappa^{0.64}, \qquad (4)$$

The RMSE is 15.8% and there is no apparent difference between the divertor and limiter data. The scaling predicts 2.1s for ITER. The scaling expression in Eq.(4) is $\propto \tau_B\ \rho_*^{\ 0.15}\ \beta^{-1.41}\ \nu_*^{\ 0.19}$ which shows it is a Bohm like scaling. From a comparison of Eq.(3) with the ELMy H-mode data, it is also apparent that the H-mode enhancement factor tends to increase with machine size.

4. ELMY H-MODE CONFINEMENT

The new public version (DB3v5p) of the ITER H-mode confinement database, ITERH.DB3, was released 1st of June 1998. This version contains data from 12 tokamaks: Alcator C-Mod (C-Mod), ASDEX, ASDEX Upgrade (AUG), COMPASS-D, DIII-D, JET, JFT-2M, JT-60U, PBX-M, PDX, TCV and TEXTOR. The new H-mode data specific to DB3v5p are detailed in [4].

The new ELMy H-mode standard dataset of DB3v5p (1398 obs. From 11 Tokamaks) [4] is significantly larger than the IAEA 1992 ELMy standard dataset (833 obs. from 6 Tokamaks) [10]. Only 3 correlation coefficients (ρ_{IP}, $\rho_{I\varepsilon}$ and $\rho_{I\kappa}$) are now larger than 0.7 and the principal components have changed significantly. The extrapolation to ITER is now only larger than 4 standard deviations around the largest principal component. The factor $\sqrt{1+\sum\lambda^2}$ in the classical statistical interval formula [11] is ~ 40% lower compared to that of DB2 implying that the log-linear interval for the ITER prediction is significantly reduced. The ELMy H-mode data now satisfies the Kadomtsev constraint [9] which was not supported earlier because the required changes to the exponents of n, B and/or R were too large. The addition of C-Mod data is responsible for the dataset now meeting the Kadomtsev constraint. The reason for this is being investigated (e.g. a reduction in the correlation between B and R may be playing a role). The new dataset is quite robust in the sense that the log-linear regression results and subsequent ITER predictions do not change appreciably if the dataset is perturbed. The Kadomtsev constrained log-linear scaling with the lowest RMSE (15.64%) is obtained with the TAUC93 renormalisation [12]. The renormalisation attempts to normalize the few closed divertor configurations represented in the database to open divertor configurations, the majority configuration represented in the database. This expression is $\propto \tau_B\ \rho_*^{-0.98}\beta^{-0.50}\nu_*^{-0.10}$, ie. a gyro-Bohm scaling, and is practically identical to the EPS97P(y) scaling [13]. The ITER prediction is 6.15s. The scaling obtained without any renormalisation is $\propto \tau_B\ \rho_*^{-1.15}\beta^{-0.37}\nu_*^{-0.12}$ which predicts 7.08s for ITER. It is the ASDEX normalisations that make the β degradation stronger and reduce the $\rho*$ dependence that leads to the lower ITER prediction. The scaling is $\propto \tau_B\ \rho_*^{-0.68}\beta^{-0.50}\nu_*^{-0.12}$ if only the ASDEX normalisations are applied and the prediction is 5.75s for ITER. With TAUC92 [10] or TAUC93 applied only to the PDX data, the regression gives $\tau_{fit} \propto \tau_B\ \rho_*^{-1.32}\beta^{-0.36}\nu_*^{-0.11}$ or $\tau_{fit} \propto \tau_B\ \rho_*^{-1.49}\beta^{-0.36}\nu_*^{-0.11}$, respectively. Hence, the PDX normalisations counteract the effect of the ASDEX normalisations on the $\rho*$ dependence. Scalings based on TAUC92 are slightly more conservative in the prediction for ITER than those based on TAUC93. The IPB98(y) scaling expression [4] is based on TAUC92 and reads (in units of s, MA, T, MW, 10^{19} m^{-3}, AMU, m, -, -):

$$\tau_{th}^{IPB98(y)} = 0.0365\ I^{0.97}\ B^{0.08}\ P^{-0.63}\ n_{19}^{0.41}\ M^{0.20}\ R^{1.93}\ \varepsilon^{0.23}\ \kappa^{0.67}, \qquad (4)$$

Eq.(4) is $\propto \tau_B \rho_*^{-0.83}\beta^{-0.50}\nu_*^{-0.10}$ and predicts 6s for ITER. The RMSE is 15.8%. In [6] uncertainties of the exponents for the individual dimensionless physics variables have been estimated by a mapping of the RMSE minima from a series of constrained regressions. Two constraints are applied: the Kadomtsev constraint plus a constraint corresponding to a given value, y, of the exponent of one other dimensionless parameter. The 95% confidence interval $\pm\ \delta y$ can then be estimated from the plot of RMSE versus y. For Eq.(4) the values of δy are 0.27, 0.24 and 0.08 for ρ_*, β and ν_*, respectively. Finally in [4] also fits using another definition of elongation, κ = area / (πa^2), which seems appropriate to use for the indented, bean shaped PBX-M and also START [14] can be found.

Based on the log-linear scalings obtained from various subsets of the data [4], the 95% log-linear interval estimate for the ELMy H-mode confinement time in ITER is (4.4–6.8 s). This comes close to a classical statistical 95% interval estimate based on the log-linear fit using TAUC92, allowing for a multiplication factor of 2 to roughly account for some of the modeling imperfections. Several non-linear scalings with lower RMSE's than that of the log-linear scalings have been found [4, 15, 16]. Allowing for these non-linear models and a number of additional considerations as presented in [4], the 95% non-linear interval estimate is (3.5–8 s). Hence, the 95% log-linear interval corresponds roughly to a 66% non-linear interval estimate (Fig.2).

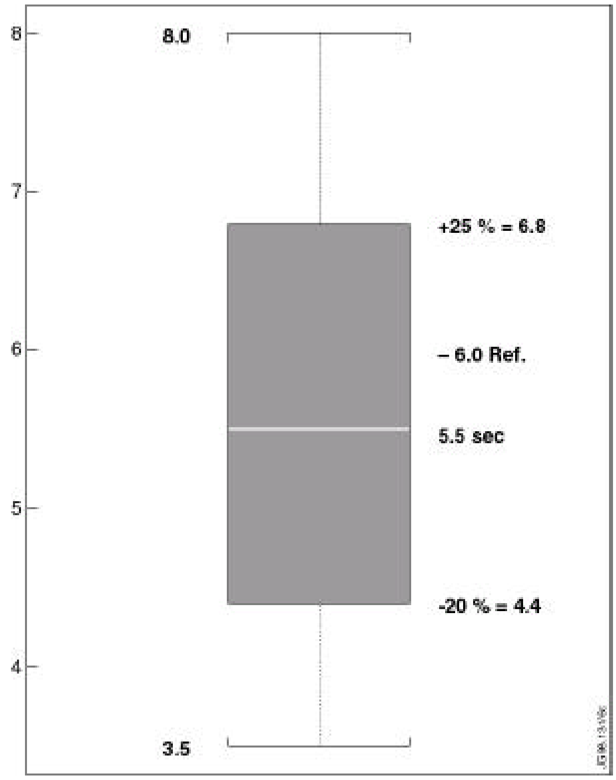

Fig. 2. Interval estimates of the confinement time in ITER at the standard operating point.

REFERENCES

[1] RYTER, F., et.al., Nucl. Fusion **36** (1996) 1867.
[2] KAYE, S., et.al., Nucl. Fusion **37** (1997) 1303.
[3] THOMSEN, K., et.al., Nucl. Fusion **34** (1994) 131.
[4] "ITER Physics Basis" Chapter II, submitted to Nucl. Fusion (1998).
[5] MARTIN, Y., et.al., Proc. 25th Eur. Conf., Prague, 1998.
[6] VALOVIC, M. et.al., Proc. 25th Eur. Conf., Prague, 1998.
[7] ITER CONFINEMENT DATABASE AND MODELING GROUP (presented by T. Takizuka), Fusion Energy 1996 (Proc 16th International Conference, Montreal, Canada), **2** (1996) 795.
[8] RIGHI, E., et.al., Submitted to Nucl. Fusion (1998).
[9] KADOMTSEV, B.B., Sov. J. Plasma Phys. **1** (1975) 295.
[10] ITER H-MODE DATABASE WORKING GROUP, (presented by O.J.W.F. Kardaun), Plasma Phys. Control. Nucl. Fus. Res. (Proc. 14th Int. Conf., Wurzburg, 1992), **3** (1993) 251.
[11] CHRISTIANSEN, J.P., et.al., Nucl. Fusion **32** (1992) 291.
[12] SCHISSEL, D.P., et.al., Proc. 20th Eur. Conf., Lisbon, 1993), Vol. 17C, Part I, 103.
[13] CORDEY, J.G., et.al., Plasma Phys. and Control Fusion **39** (1997) B115.
[14] ROBINSON, D., et.al., To appear in Plasma Phys. Control. Fusion (1998).
[15] KARDAUN, O.J.W.F., et.al., Proc. 21st Eur. Conf., Montpellier, 1994), Vol. 18B, Part I, 90.
[16] TAKIZUKA, T., Plasma Phys. Control. Fusion **40** (1998) 851.